Removal of Mixed Cationic Dyes by a Biosorbent Based on Magnetic Tragacanth Gum Hydrogel

Jaymand, Mehdi*[+]

Nano Drug Delivery Research Center, Health Technology Institute,
Kermanshah University of Medical Sciences, Kermanshah, I.R. IRAN

ABSTRACT: *A magnetic tragacanth gum-grafted poly(acrylic acid) hydrogel (TG-g-PAA/Fe_3O_4) was applied for the removal of Malachite Green (MG), basic yellow 28 (BY28) and rhodamine 6G (Rh6G) dyes form industrial simulated wastewater. The most important parameters (e.g., initial dye concentrations, adsorbent dosage, pH, and contact time) were optimized in all single, binary, and ternary systems. The adsorption processes were better fitted with the Langmuir model than the Freundlich model which revealed the linearity of the processes. Maximum adsorption capacities (Q_m) for MG, BY28, and Rh6G in the ternary system were obtained as 626.5, 568.2, and 459.7 mg/g, respectively. Kinetic studies exhibited that the removal of all dyes in all systems was best fitted with the pseudo-second-order model, which proved the rate-limiting step might be the chemical adsorption. The hydrogel was regenerated by the desorption process after the loading process and reused several times. As a result, the removal efficiency of the adsorbent almost remains the same for the first four cycles.*

KEYWORDS: *Natural hydrogel; Magnetic nanoparticles; Synthetic dye; Simultaneous removal; Adsorption.*

INTRODUCTION

Nowadays, water pollution caused by synthetic dyes has become a global concern. Synthetic dyes are used annually in different industries such as plastics, textiles, leather, paper, and dyestuff because of their coloring properties. These are toxic, non-degradable, bio-accumulative, mutagenic, and carcinogenic which cause serious health issues for humans, aquatic fauna, and flora [1-5]. Wastewater containing synthetic dyes impedes sunlight penetration and upsets the photosynthetic activity of aquatic life. Also, it leads to dermatitis, allergy, and skin irritation as well as carcinogenic agents. Consequently, the treatment of wastewater containing these dyes is of high importance [6, 7]. Various methods have been used for the removal of dyes from wastewater, including membrane filtration [8], adsorption [9], ion exchange [10], photocatalytic [11], coagulation [12], Advanced Oxidation Process (AOP) [13], electrochemical [14], and biological methods [15]. The advantages and disadvantages of the mentioned approaches are listed in Table 1. Among them, the adsorption method has been widely applied for dye removal because of its simplicity, high efficiency, low cost, and reusability features [9]. Various types of adsorbents such as graphene

**To whom correspondence should be addressed.*
+ *E-mail: m_jaymand@yahoo.com*
• *Other address: Student Research Committee, Kermanshah University of Medical Sciences, Kermanshah, I. R. IRAN.*
1021-9986/2023/8/2670-2686 17/$/6.07

Table 1: The advantages and disadvantages of various pollutants removal methods

Method	Advantages	Disadvantages
Ion change	Stability of adsorbent	High cost, and unsuitable to some dyes
Adsorption	High performance, simplicity, low cost, and re-usability	Unsuitable to some dyes, and the disposal of used adsorbent
Membrane separation	High performance, and re-usability	Short life-time, and high cost
Coagulation	Simplicity, and low cost	High sludge generation, and disposal problems
Electrochemical process	High performance, and rapid operation	High energy consumption, and high cost
Advanced oxidation process	High performance, and rapid operation	Sludge generation, high cost, high reagents and energy consumption, and by-products creation
Photochemical process	No sludge generation, and rapid operation	By-products creation, and energy consumption
Biodegradation	Low cost, and facile	Environmental conditions issues, and slow process

oxide/manganese dioxide (GO/MnO_2) [16], activated carbon [17], multi-functionalized fibrous silica (MF-KCC-1) [18], nitrilotriacetic acid β-cyclodextrin-chitosan (NTA-β-CD-CS) [19], polyaniline@zinc oxide (PANI@ZnO) [20], mesoporous materials [21, 22], and Metal–Organic Framework (MOF) [23] have been reported for the removal of dyes from wastewater.

Hydrogels are another category of potent sorbent for the removal of synthetic dyes owing to their excellent physicochemical properties, including swelling in aqueous media up to several times, colorlessness, odorlessness, non-toxicity, excellent environmental stability, and low production cost in most cases [24-28]. Amongst, natural polymers-based hydrogels have been received more and more attention due to their superior physicochemical as well as biological features that lead to numerous biological as well as industrial applications [25, 29-31].

Tragacanth Gum (TG), an acidic polysaccharide, is a biocompatible and biodegradable natural polymer. TG achieves in two different forms containing ribbon and flake. Availability, high thermal and environmental stability, cheap, non-toxicity, and eco-friendly are some of the advantages of this natural gum [32, 33]. TG is frequently applied in various fields, including pharmaceuticals [21], food and cosmetics industries [34], emulsifier [35], fat replacer [36], and cross-linking agent [37]. TG composed mainly from branched acidic hetero-polysaccharides of D-galacturonic acid. Sugars include D-galactose, L-fucose (6-deoxy-L-galactose), D-xylose and L-arabinose generated after its hydrolysis. TG is composed of two fractions of water-soluble and insoluble, so that tragacanthin (30–40 %) act as the soluble fraction to create a viscous colloidal hydrosol, while bassorin (60–70%) act as the insoluble fraction to form a stiff gel [38]. The hydroxyl and carboxylic acid groups in TG backbone provide the proper opportunity for reacting with cross-linking reagents and chemical modification [39]. In this context, grafting of synthetic polymers (*e.g.*, poly(acrylic acid); PAA) can improve some physicochemical properties of the resultant hydrogel for its final usage aim. Some research projects have been conducted for the removal of organic dyes using TG-based hydrogels. For example, Sadeghi et al. applied a nanocomposite containing TG and poly(methyl methacrylate) (PMMA) reinforced with bentonite for the removal of acid blue 113 (AB-113), methyl orange (MO), and congo red (CR) dyes [40]. In another study, Mallakpour et al. synthesized TG/$CaCO_3$@EDTA nanocomposite for the adsorption of methylene blue (MB) dye [41].

Incorporation of Fe_3O_4 nanoparticles (NPs) into the hydrogel-based sorbent have been attracted a great deal of interest due to simple separation of magnetic hydrogels from aqueous solution by using a magnetic field. Magnetic hydrogels-based adsorbents have been used for various pollutants removal, including dyes [42], heavy metals [43], phosphate [44], ammonia [45], and pesticide [46].

As the above-discussion, present study was aimed at application of a TG-*g*-PAA/Fe_3O_4 magnetic hydrogel as a biosorbent for efficient removal of rhodamine 6G (Rh6G), basic yellow 28 (BY28), and malachite green (MG) dyes from single, binary, and ternary systems (Figs. 1 and 2). The effects of different parameters such as pH, contact time, initial dye concentration, and sorbent dosage were studied and optimized.

EXPERIMENTAL SECTION

Materials

The magnetic hydrogel (TG-*g*-PAA/Fe_3O_4) was synthesized in our laboratory [47]. The MG, Rh6G and BY28 cationic dyes were obtained from (Sigma-Aldrich,

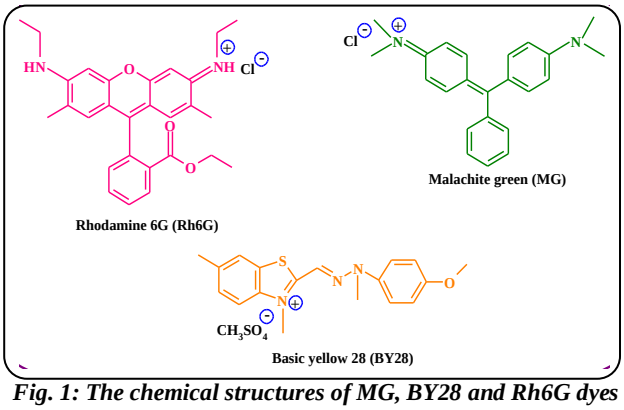

Fig. 1: The chemical structures of MG, BY28 and Rh6G dyes

St. Louis, MO, USA). Sodium hydroxide (NaOH), hydrogen chloride (HCl), sodium carbonate ($NaCO_3$), and sodium chloride (NaCl) were provided from Sigma-Aldrich.

Swelling properties

The swelling properties of the TG-*g*-PAA/Fe_3O_4 hydrogel was assessed by the well-established gravimetric method. For this aim, the dried hydrogel was cut and weighed. The species were immersed in deionized water and weighed at the predetermined time intervals. The swollen species were taken out, the additional water on the surface was removed using a filter paper, and weighed again. The swelling (SR) percent was quantified by the following equation.

$$SR\ (\%) = \frac{W_t - W_i}{W_i} \times 100 \qquad (1)$$

where, W_t is weight of swelled hydrogel at time t, and W_i is the initial weight of the hydrogel [48].

Zero point charge (pH_{zpc}) of TG-g-PAA/Fe_3O_4 hydrogel

In adsorption process, removal efficiency is significantly depends on the zero point charge (pH_{zpc}) of adsorbent. For investigation the pH_{zpc} value of the adsorbent, NaCl solution (30 mL; 0.1 $molL^{-1}$) were added to Erlenmeyer flasks, and pH of solutions were adjusted between 1 to 9 using dilute solution of NaOH or HCl (0.1 $molL^{-1}$). The preliminary pH values were denoted as pH_i. Afterward, the sorbent (0.10 g) was added to each flask, and stirred till no variation in pH values was observed between two successive readings. The equilibrium pH (pH_e), which was used to calculate ΔpH (pH_i–pH_e). Graph of ΔpH against pH_i gave the pH_{zpc} value at which the ΔpH reads zero (Fig. 4) [49, 50].

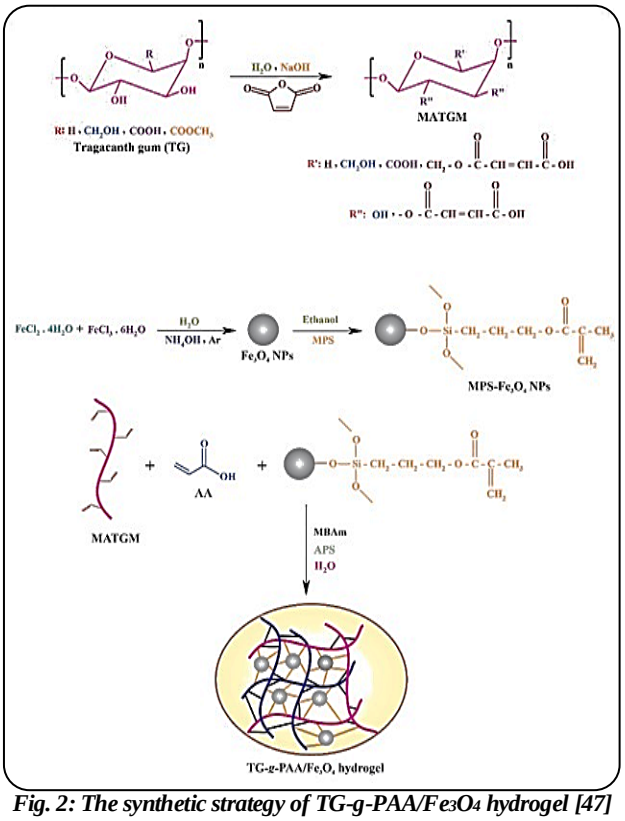

Fig. 2: The synthetic strategy of TG-g-PAA/Fe_3O_4 hydrogel [47]

Adsorption processes

Single dye system

The well-established batch approach was used for the removal of MG, BY28 and Rh6G cationic dyes. In a typical experiment, the TG-*g*-PAA/Fe_3O_4 hydrogel was immersed in 100 mL solutions of MG, BY28 and Rh6G dyes with concentration of 100 to 700 mg/L. The pH of solutions were adjusted in the range of 3 to 9 through the addition of HCl or NaOH solutions (0.1 mol/L). The removal processes were performed at contact times of 10-120 minutes. The sorbent dosage was optimized using 1, 2, 4, 6, 8, 10 g/L of hydrogel. The industrial condition was stimulated through the addition of sodium carbonate (0.003 mol/L) and sodium chloride (0.01 mol/L) to the dyes solutions. The removal efficiency (R) and equilibrium adsorption capacity (q_e) of the sorbent were calculated using a UV-vis spectrophotometer (at 618, 528 and 439 nm for MG, Rh6G and BY28, respectively) by Equations (2) and (3), respectively.

$$R(\%) = \frac{(C_o - C_e)}{C_o} \times 100 \qquad (2)$$

$$q_e = \frac{(C_o - C_e)}{W} \times V \qquad (3)$$

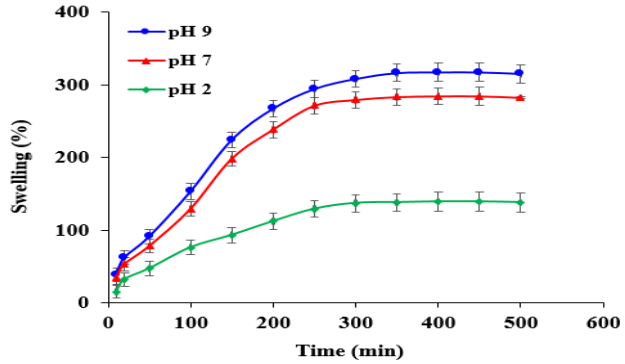

Fig 3. Swelling behavior of TG-g-PAA/Fe3O4 hydrogel at pH 2, 7 and 9.

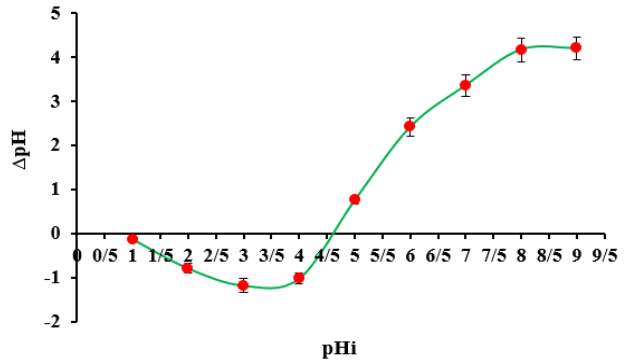

Fig. 4: The pH_{zpc} value for the TG-g-PAA/Fe_3O_4 hydrogel

where, C_o (mg/L) and C_e (mg/L) are the initial and final concentrations of each dye, respectively, V is the dye solution volume (mL), and W is the mass of sorbent (g) [51, 52].

Binary dyes system

In a binary removal system, 100 mL (400 mg/L) of dyes solutions taken for experiment at optimized condition. The removal efficiency for each dye was calculated by a UV-vis spectrophotometer using equations 2 and 3.

Ternary dyes system

In ternary system, 33.33 mL (400 mg/L) of each dye was taken for process under optimized condition. The concentrations of each dye was quantified by a UV-Vis spectrophotometer using equations 2 and 3.

Regeneration and reusability

The dye(s) loaded TG-*g*-PAA/Fe_3O_4 sorbent was immersed in various solvents at various pH's (3 to 10) and stirred in ambient condition. Consequently, the hydrogel was isolated by an external magnet bar, and the dyes concentration were calculated by a UV-Vis spectrophotometer according to Equation (4).

$$\text{Desorption } (\%) = \frac{C_e}{C_o} \times 100 \qquad (4)$$

Where, C_o (mg/L) and C_e (mg/L) are the initial and final concentrations of dye(s), respectively. The regenerated TG-*g*-PAA/Fe_3O_4 hydrogel was taken for adsorption-desorption process under optimized condition for several times.

Characterization

The Ultraviolet-visible spectra were provided using a Specord 210 Plus spectrophotometer (Analytik-Jena AG, Germany).

RESULTS AND DISCUSSION

Swelling behavior

The swelling properties of the TG-*g*-PAA/Fe_3O_4 hydrogel was investigated in numerous pH values (2, 7, and 9) as depicted in Fig. 3. During swelling, the volume of the sorbent increased significantly that can improve dyes uptake significantly. As seen, by increasing time in all pH values the swelling was increased, and after 350 min the swelling reached equilibrium. In addition, increasing the pH value lead to increasing the swelling. The highest swelling was obtained as 316% after 350 min at pH 9.

The pH_{zpc} measurement

The pH_{zpc} value for the TG-*g*-PAA/Fe_3O_4 hydrogel was measured as 4.65. Consequently, the surface of the TG-*g*-PAA/Fe_3O_4 adsorbent will be negatively charged above pH_{zpc} and positively charged below pHzpc. Therefore, TG-*g*-PAA/Fe_3O_4 hydrogel can be easily adsorb cationic dyes at pH values higher than 4.65 due to efficient physical interactions between dyes and hydrogel matrix (Fig. 4).

Removal condition optimization

The most important parameters, including pH, initial dye concentration, adsorbent dosage, and contact time that influence removal process were optimized as follows.

Effect of pH

The effect of pH on removal efficiency of MG, Rh6G and BY8 dyes were studied in single, binary, and ternary

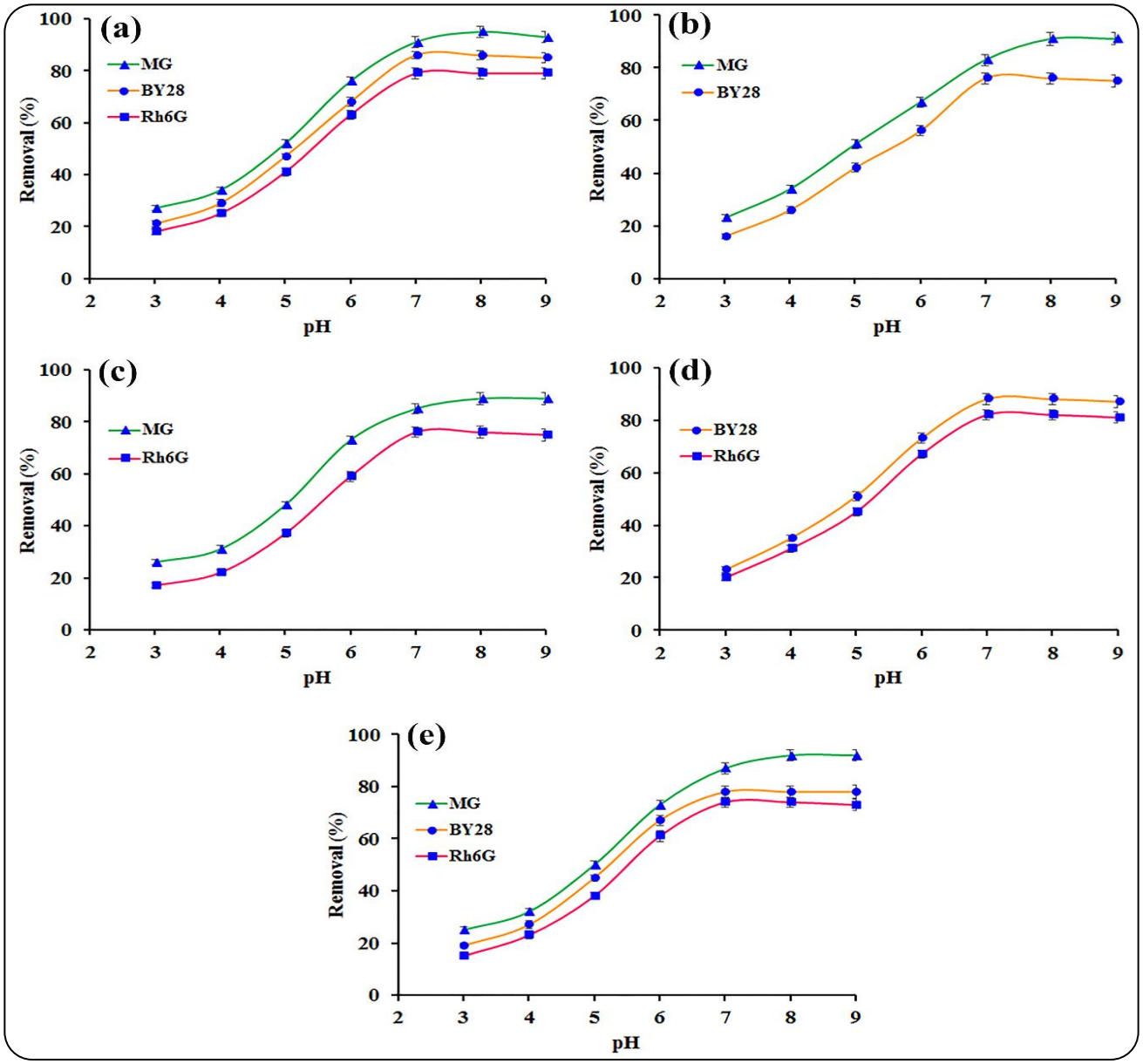

Fig. 5: The effect of pH on the removal efficiencies of MG, BY28 and Rh6G dyes in single (a), binary (b, c, and d), and ternary (e) systems (condition: 25 °C; dye concentration 400 mg/L, adsorbent dosage 8 g/L, and contact time 90 minutes)

systems in the range of 3 to 9 as depicted in Fig. 5. As expected, at acidic pH values (especially below pH_{zpc}; 4.65) the sorbent did not showed acceptable removal efficiency owing to its positively charged surface. In contrast, above pH_{zpc} removal efficiency was increased in all systems for all dyes due to excellent physical interactions (*e.g.*, ionic and hydrogen bonding) between dyes and hydrogel matrix.

In single system (Fig. 5**a**), the highest removal efficiencies for MG (95%), Rh6G (79%), and BY28 (86%) were obtained at pH 8, 7 and 7, respectively. In binary system composed of MG and BY28 dyes, the highest removal efficiencies were obtained as 91 and 76%, respectively, at pH 8 and 7, respectively (Fig. 5**b**). In MG and Rh6G binary system, the highest removal efficiencies were obtained as 89 and 76%, respectively, at pH 8 and 7, respectively. The optimal pH value for the removal of BY28 (88%) and Rh6G (82%) dyes in binary system was obtained as 7 for both dyes. In the case of this binary system, hydrogen bonding between the dyes as well as matrix and π-π stacking between dyes lead to higher removal efficiency than those of the other systems.

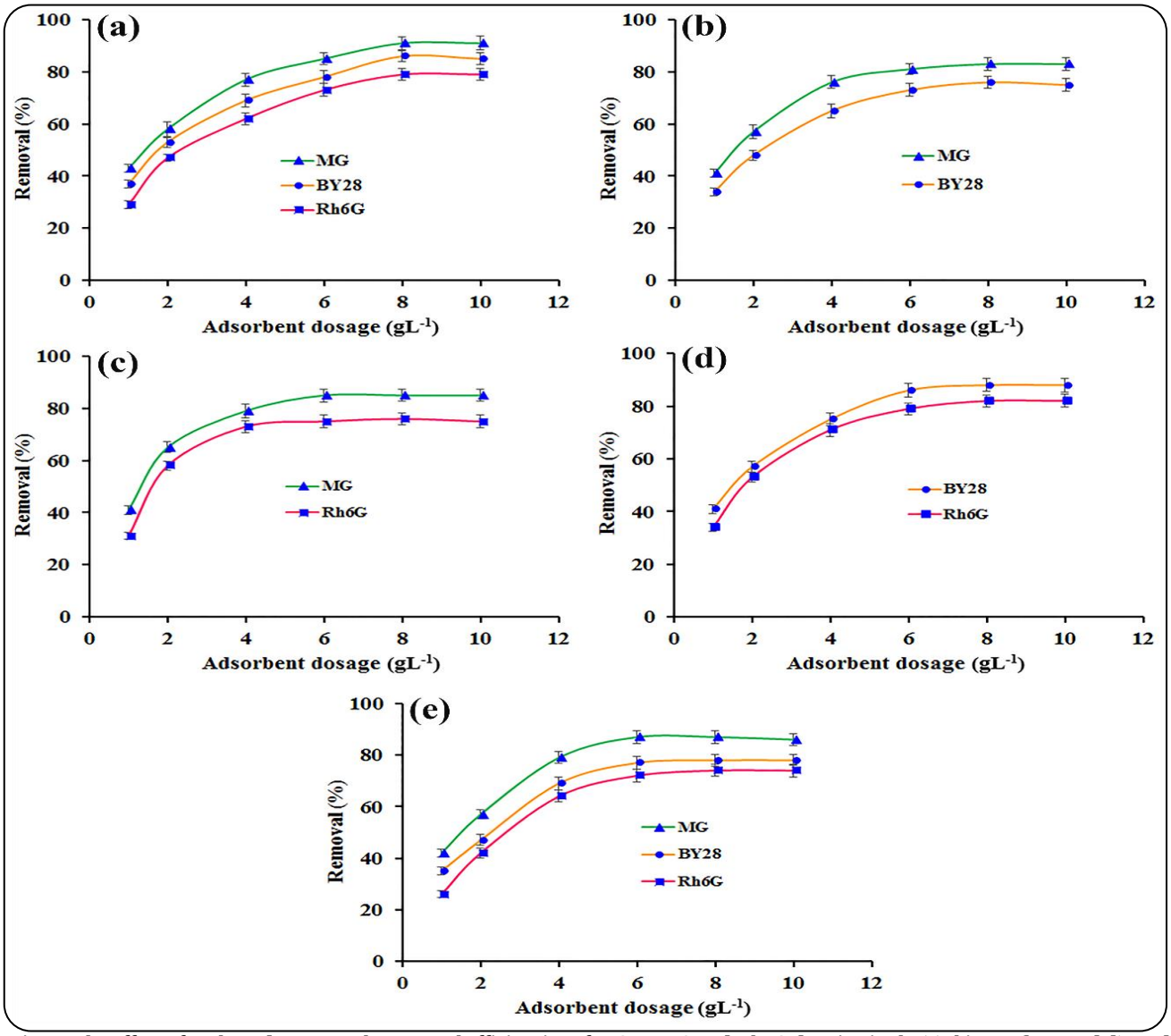

Fig. 6: The effect of sorbent dosage on the removal efficiencies of MG, BY28 and Rh6G dyes in single (a), binary (b, c, and d), and ternary (e) systems (condition: 25 °C; pH 7; dye concentration 400 mg/L; and contact time 90 minutes)

Finally, in ternary system the optimal pH value for the removal of MG (92), BY28 (78%) and Rh6G (74%) dyes were obtained 8, 7, and 7, respectively. As the results, pH 7 was selected as the optimal pH value for all dyes and systems.

Effect of adsorbent dosage

In adsorption process, adsorbent dosage optimization is an important stage owing to commercial and environmental aspects of views. The effect of adsorbent dosage on removal efficiencies of MG, BY28 and Rh6G dyes was studied in single, binary, and ternary systems as illustrated in Fig. 6.

The removal efficiencies of all dyes were increased continuously with the increasing of adsorbent dosage up to 8 g/L in all single, binary, and ternary systems, and after which the removal efficiencies did not changed significantly. The maximum removal of MG, BY28 and Rh6G dyes in optimum sorbent dosage (8 g/L) were obtained as 91, 86, and 79%, respectively, in single system Fig. 6**a**). As seen in Fig. 6**b**, in MG and BY28 binary system the maximum removal were obtained as 83 and 76%, respectively.

In MG and Rh6G binary system, the maximum removal were obtained as 85 and 76%, respectively (Fig. 6**c**). In BY28 and Rh6G binary system, the maximum removal were quantified

as 88 and 82%, respectively (Fig. 6**d**). Finally, in MG, BY28 and Rh6G ternary system, the maximum removal were calculated to be 87, 78, and 74%, respectively (Fig. 6**e**). As the results, the optimum sorbent dosages for all single, binary, and ternary systems was selected as 8 g/L for all dyes.

Effect of initial dye concentration

In general, the wastewater containing dyes was concentrated before treatment. Therefore, the optimization of initial dyes concentrations is particular of interest in adsorption processes. As seen in all single, binary and ternary systems, the sorbent can be adsorb approximately 100% of dyes up to concentration of 300 mg/L under optimized condition. In contrast, at higher concentrations, the saturation of the adsorbent active sites led to lower quantities of dyes adsorption. As the high concentration of wastewater and acceptable removal efficiency of dyes up to concentration of 400 mg/L, this concentration was selected as the optimal value for all dyes in all systems.

In detail, the adsorbent can be remove 91, 86 and 79% of MG, BY28 and Rh6G dyes, respectively, at concentration of 400 mg/L in single system (Fig. 7**a**). In MG and BY28 binary system, the removal efficiencies at dyes concentration of 400 mg/L were quantified as 83 and 76%, respectively (Fig. 7**b**). In binary system composed of MG and Rh6G dyes, the sorbent can adsorb 85 and 76% of dyes, respectively (Fig. 7**c**). The removal efficiency of BY28 and Rh6G dyes at optimal concentration were calculated to be 88 and 82%, respectively (Fig. 7**d**). Finally, at the ternary system, the removal efficiencies of MG, BY28 and Rh6G dyes at concentration of 400 mg/L were obtained as 87, 78, 74%, respectively (Fig. 7**e**).

Effect of contact time

The effect of contact time on removal efficiencies of MG, BY28 and Rh6G dyes in all single, binary, and ternary systems were investigated and the results obtained are summarized in Fig. 8. As seen, the highest removal efficiencies for all dyes in all systems (except MG in single system; 80 minutes) were obtained to be 90 minutes, and after which the removal efficiency of each dye is not changed significantly. Therefore, 90 minutes was selected as the optimum contact time for all dyes in all systems.

Time-dependent removal process

Time-dependent removal of MG, BY28 and Rh6G dyes in single, binary, and ternary systems were performed on the above-mentioned optimal condition, and electronic spectra as well as photographs are illustrated in Figs. 9, 10, and 11.

Adsorption isotherms

Langmuir and Freundlich isotherm models were applied for adsorption isotherm study in all single, binary and ternary systems at optimum condition (Equations (5) and (6), respectively).

$$\frac{C_e}{q_e} = \frac{C_e}{Q_m} + \frac{1}{Q_m K_L} \quad (5)$$

$$q_e = K_F C_e^{1/n} \quad (6)$$

In these equations, q_e (mg/g) is the adsorbed dye concentration on the sorbent, C_e (mg/L) is the equilibrium concentration of dye in the bulk solution, Q_m (mg/g) is the monolayer adsorption capacity, K_L (L/mg) is the Langmuir constant, K_F and n are the Freundlich constants.

Another important parameter in the Langmuir isotherm model is dimensionless constant (R_L; otherwise known as equilibrium parameter) that investigated by following equation [53].

$$R_L = \frac{1}{1 + a_L C_0} \quad (7)$$

In Equation (7), R_L is the shape of the Langmuir isotherm, a_L (L/mg) is the Langmuir constant associated with the energy of adsorption, and C_0 (mg/L) is the initial concentration of dyes. The a_L was obtained from the slope of the Langmuir isotherm. If $R_L > 1$, $R_L=1$, $R_L=0$, and $R_L < 1$ the adsorption process are considered as un-favorable, linear, irreversible, and favorable, respectively.

Langmuir and Freundlich isotherm plots for the removal of MG, BY28 and Rh6G dyes in single system are depicted in Fig. 12. The R^2 values for all dyes in Langmuir model are approach's to one, which revealed the Langmuir model is well-fitted in comparison with the Freundlich model to describe the adsorption process. In the case of binary (Fig. 13) and ternary (Fig. 14) systems were also obtained the similar results. These data confirm the linearity of the adsorption process.

Some Langmuir and Freundlich isotherm models parameters are summarized in Tables 2 and 3, respectively. According to R_L and 1/n values (< 1), the adsorption of all dyes onto/into the sorbent is favorable. In addition,

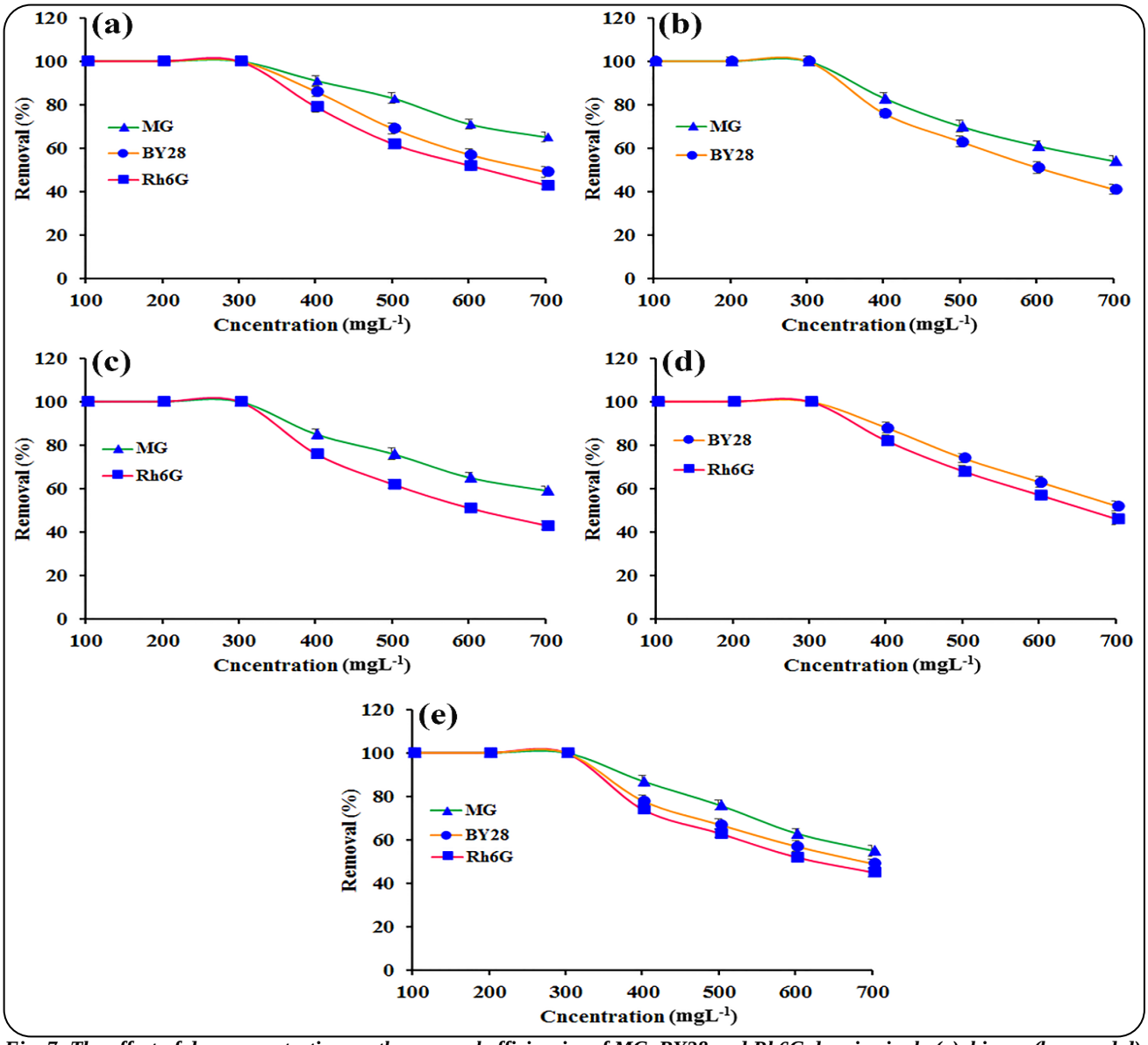

Fig. 7: The effect of dye concentration on the removal efficiencies of MG, BY28 and Rh6G dyes in single (a), binary (b, c, and d), and ternary (e) systems (condition: 25 ℃; pH 7, contact time 90 minutes, and adsorbent dosage 8 g/L)

Q_m vales for MG, BY28 and Rh6G dyes in single,binary, and ternary systems were quantified and listed in Table 2.

Adsorption kinetics

The sorption rates of MG, BY28 and Rh6G dyes onto/into the TG-*g*-PAA/Fe_3O_4 hydrogel were evaluated using pseudo-first-order and pseudo-second-order kinetic models (Equations (8) and (9), respectively).

$$\log(q_e - q_t) = \log q_e - \frac{k_1}{2.303}t \quad (8)$$

$$\frac{t}{q_t} = \frac{1}{k_2 q_e^2} + \frac{t}{q_e} \quad (9)$$

Where, q_e (mg/g) is the loaded number of dyes at the equilibrium, q_t (mg/g) is the loaded dyes amount at time *t*, k_1 and k_2 are the pseudo-first-order and pseudo-second-order equation rate constants, respectively. The kinetic study results such as correlation coefficient, k_1 and k_2 values are represented in Table 4. As seen, the adsorption of MG, BY28 and Rh6G dyes in all systems (single, binary, and ternary) are well-fitted with the pseudo-second-order model ($R^2 > 0.98$) than those of the pseudo-first-order model. As these data, the rate-limiting step might be the sorption of dyes onto/into the adsorbent, but not the mass transport.

Table 2: Langmuir isotherm model parameters at 25 ℃ for single, binary, and ternary systems

Dye(s)	Q_{max} (mg/g)	K_L (L/mg)	R_L	R^2
MG	641.7	0.148	0.0053	0.9922
BY28	583.4	0.237	0.0059	0.9896
Rh6G	473.5	0.253	0.0067	0.9864
MG+BY28	634.3/572.1	0.172/0.246	0.0055/0.0063	0.9923/0.9841
MG+Rh6G	627.6/451.3	0.18/0.268	0.0055/0.0071	0.9908/0.9837
BY28+Rh6G	591.8/479.3	0.224/0.241	0.0054/0.0062	0.9864/0.9872
MG+BY28+Rh6G	626.5/568.2/459.7	0.179/0.251/0.276	0.0057/0.0065/0.0074	0.9945/0.9945/0.9883

Table 3: Freundlich isotherm model parameters at 25 ℃ for single, binary, and ternary systems

Dye(s)	n	K_F (L/mg)	R^2
MG	4.11	178.4	0.9695
BY28	4.04	161.7	0.9574
Rh6G	3.79	152.9	0.9392
MG+BY28	4.05/4.01	172.3/154.6	0.9323/0.9309
MG+Rh6G	4.02/3.57	171.7/146.2	0.9346/0.9376
BY28+Rh6G	4.08/3.82	166.2/159.1	0.9341/0.9294
MG+BY28+Rh6G	4.01/3.94/3.48	164.1/151.3/142.72	0.9766/0.9674/0.9534

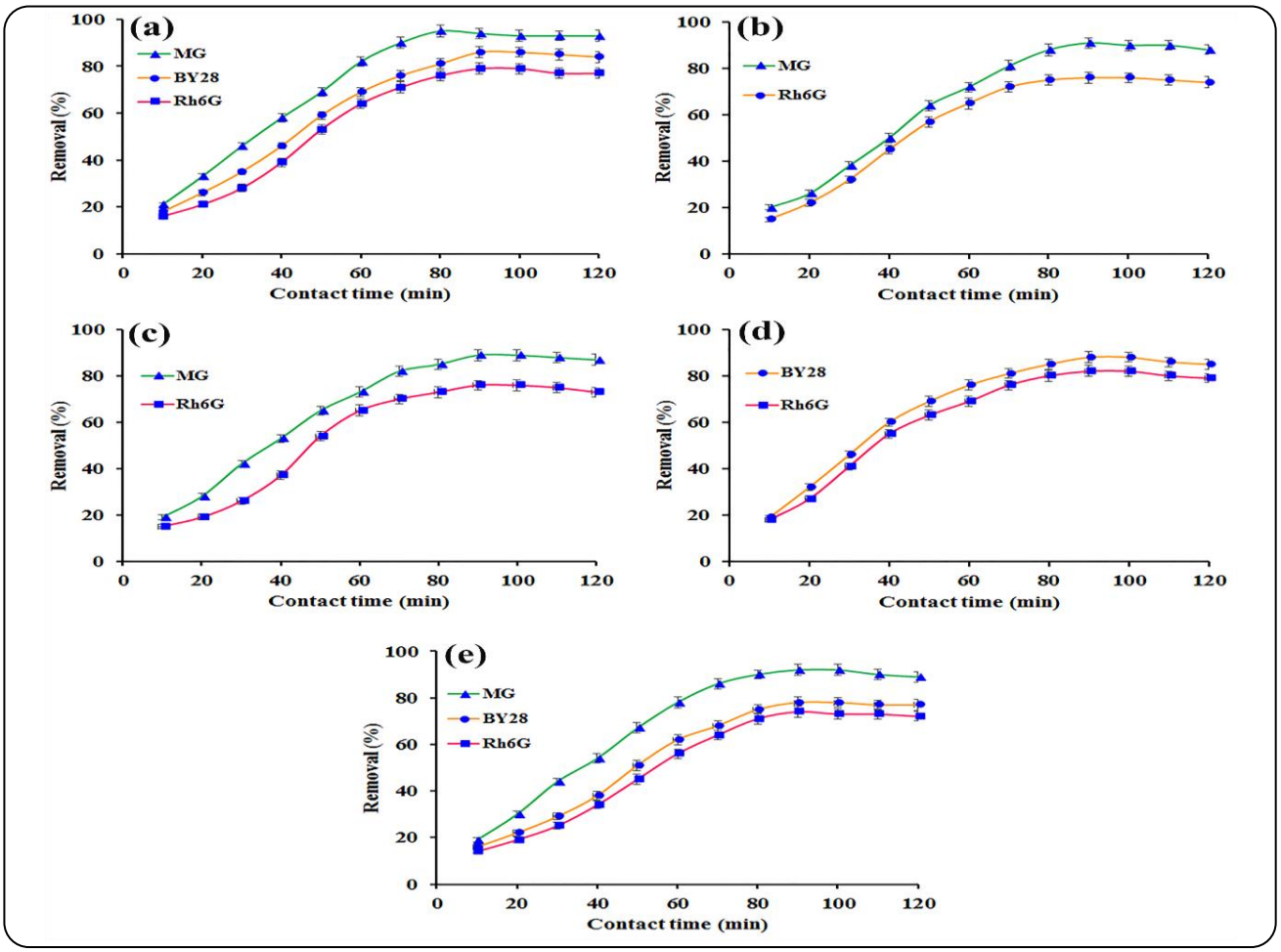

Fig. 8. The effect of contact time on the removal efficiencies of MG, BY28 and Rh6G dyes in single (a), binary (b, c, and d), and ternary (e) systems (condition: 25 °C; dye concentration 400 mg/L; pH 7, and adsorbent dosage 8 g/L)

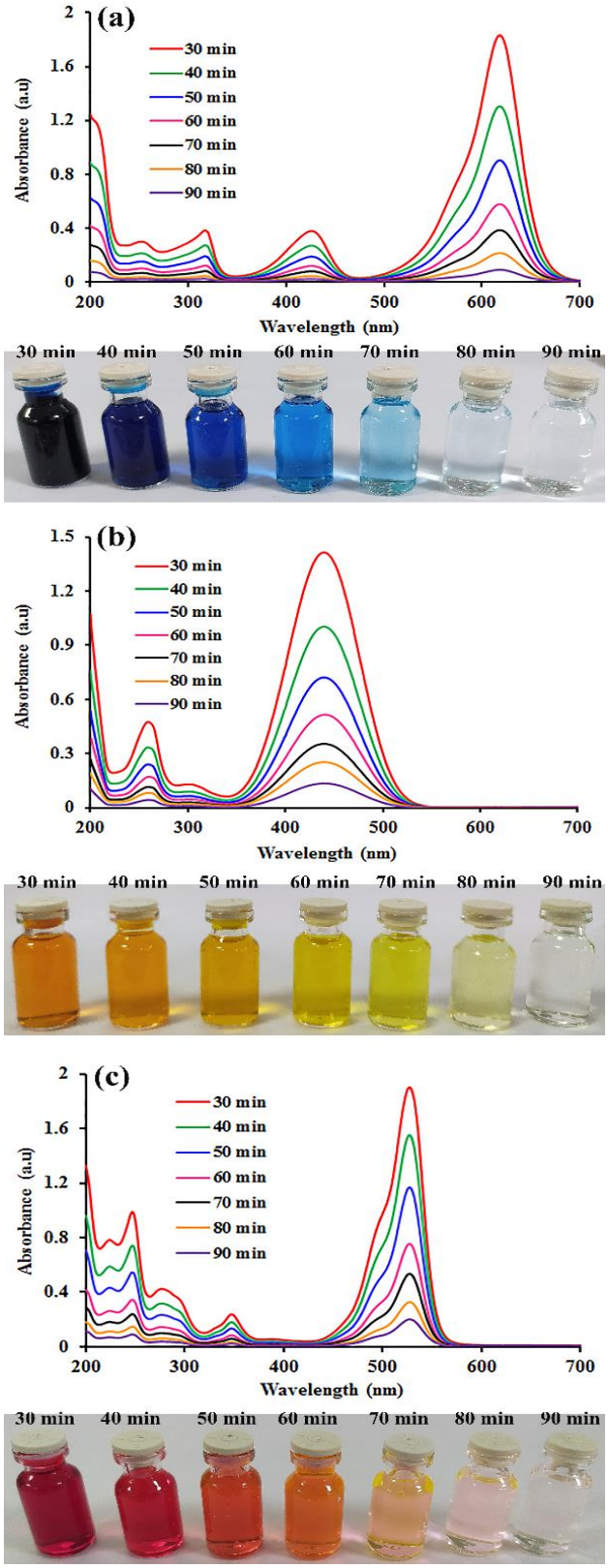

Fig. 9: Time-dependent removal of MG (a), BY28 (b), and Rh6G (c) in single system

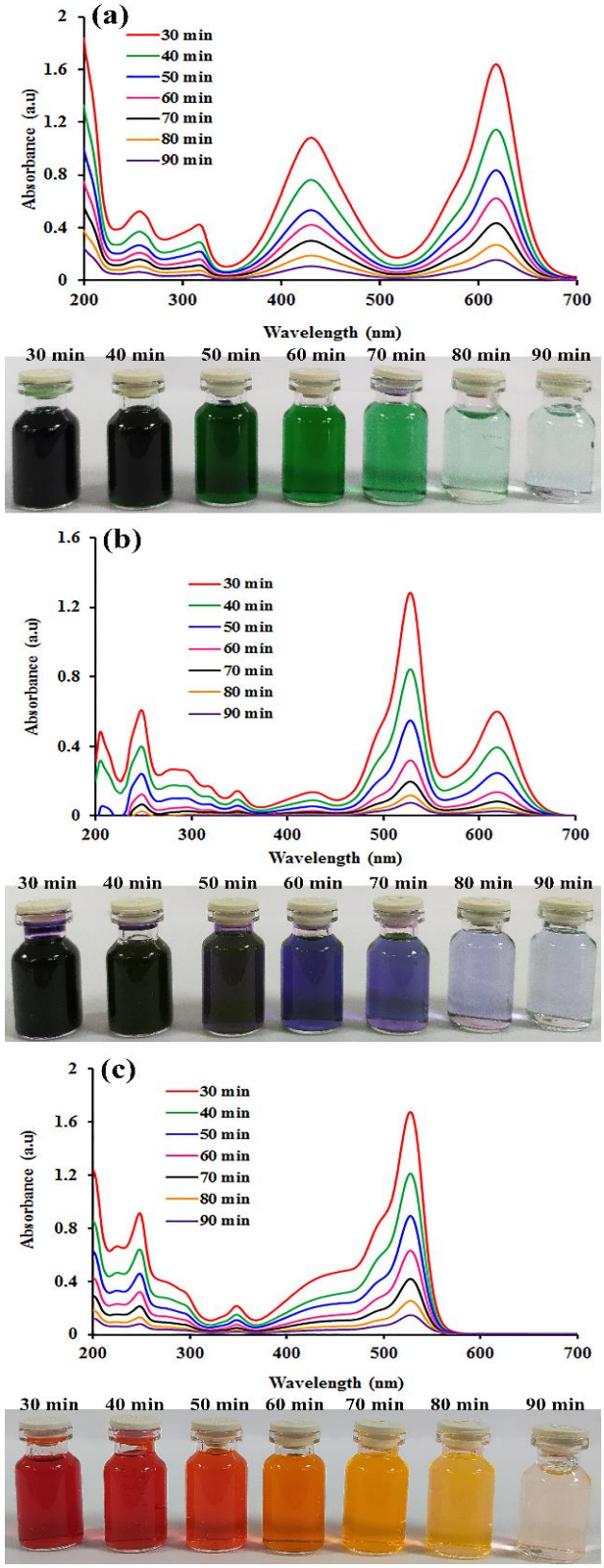

Fig. 10: Time-dependent removal of MG+BY28 (a), MG+Rh6G (b), and BY28+Rh6G (c) in binary system

Table 4: Adsorption kinetic parameters for the sorption of MG, BY28 and Rh6G dyes onto/into adsorbent in single, binary, and ternary systems

	Pseudo-first-order		Pseudo-second-order	
Dye(s)	$k_1 \times 10^{-2}$ (min^{-1})	R^2	$k_2 \times 10^{-3}$ (g/(mg.min))	R^2
MG	1.69	0.969	3.02	0.998
BY28	1.76	0.954	2.91	0.993
Rh6G	1.83	0.942	2.73	0.991
MG+BY28	1.71/1.81	0.961/0.952	2.98/2.83	0.997/0.991
MG+Rh6G	1.74/1.87	0.969/0.951	2.96/2.63	0.996/0.984
BY28+ Rh6G	1.72/1.79	0.951/0.947	2.97/2.79	0.994/0.993
MG+BY28+Rh6G	1.62/1.72/1.86	0.967/0.949/0.941	2.97/2.77/2.52	0.993/0.989/0.984

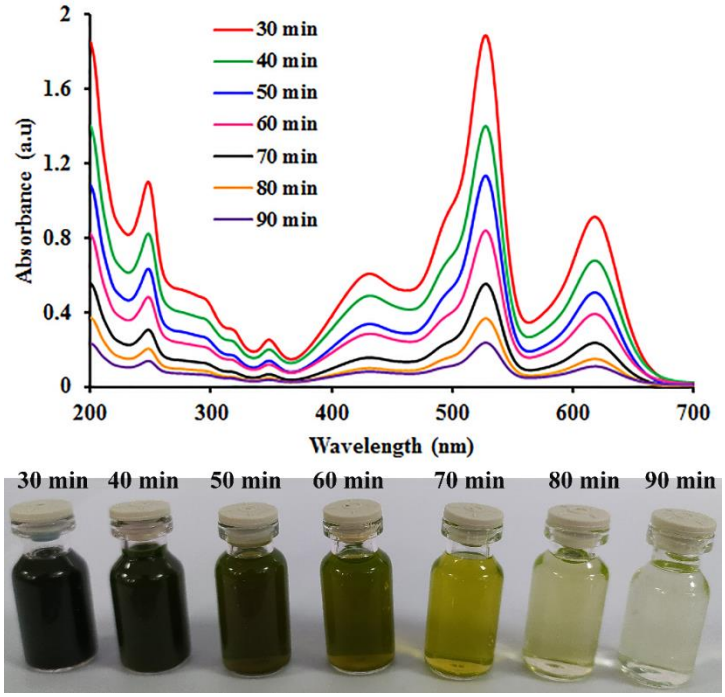

Fig. 11: Time-dependent removal of MG, BY28, and Rh6G dyes in ternary system

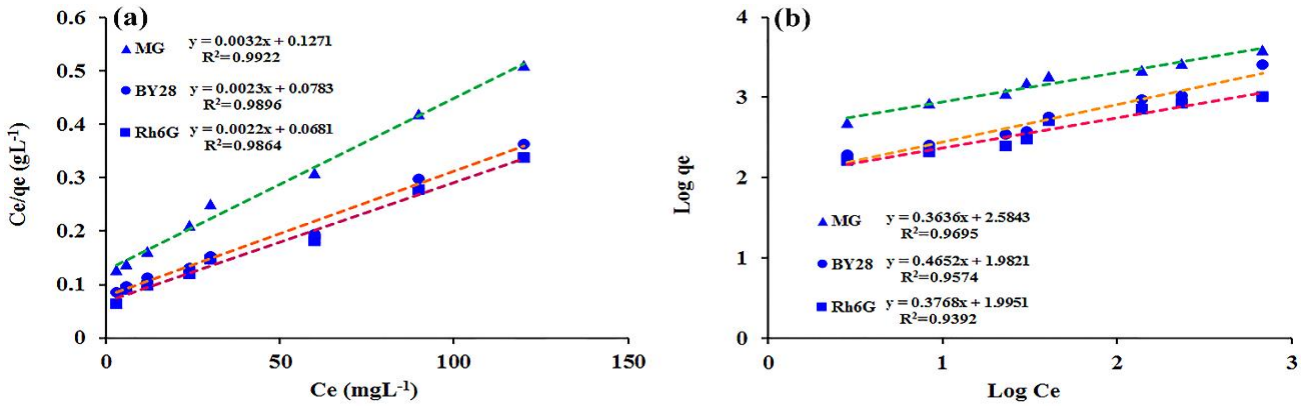

Fig. 12: Plots of Langmuir (a) and Freundlich (b) isotherm models for the sorption of MG, BY28 and Rh6G dyes in single system

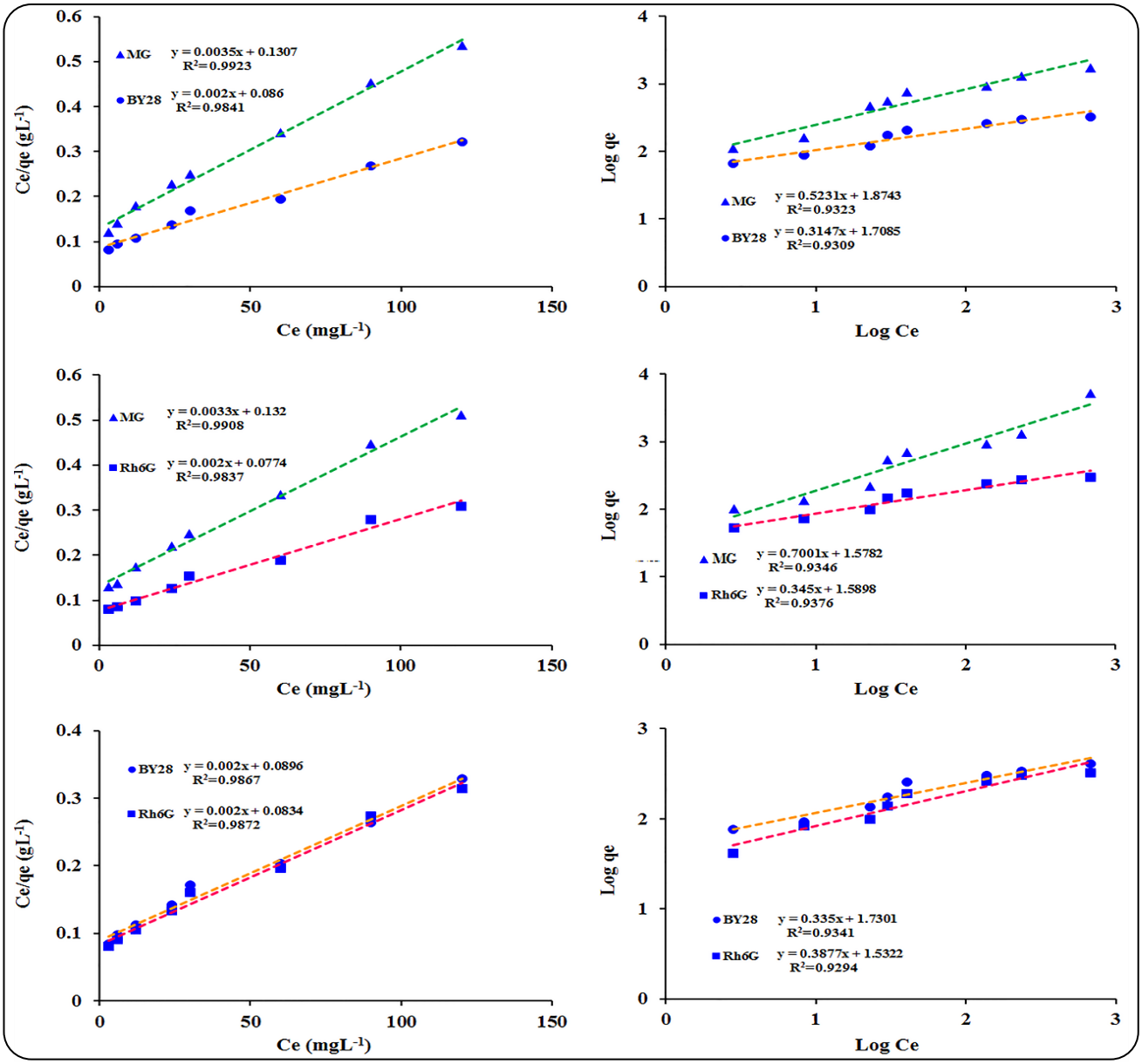

Fig. 13: Plots of Langmuir (left column) and Freundlich (right column) isotherm models for the sorption of MG, BY28 and Rh6G dyes in binary systems

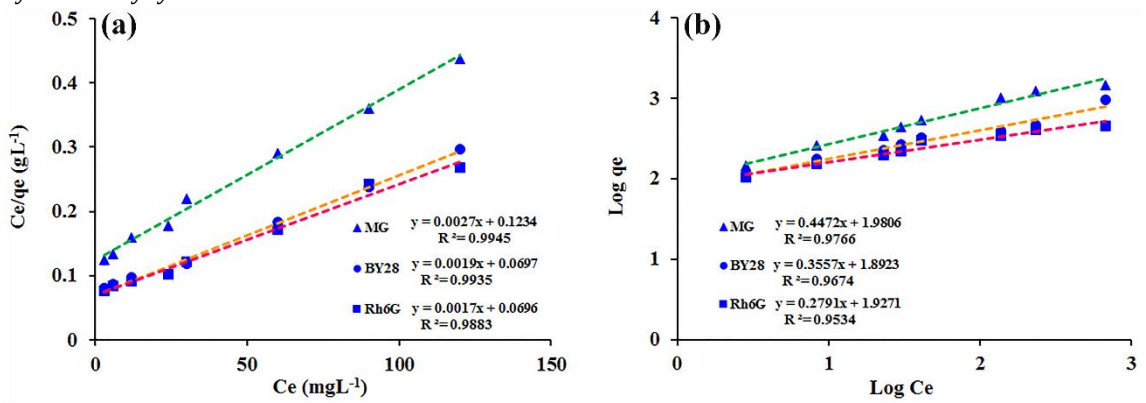

Fig. 14: Plots of Langmuir (a) and Freundlich (b) isotherm models for the sorption of MG, BY28 and Rh6G dyes in ternary system

Table 5: Desorption values of MG, BY28 and Rh6G dyes from TG-g-PAA/Fe$_3$O$_4$ hydrogel

Eluent	Desorption efficiency (%)[a]		
	MG	BY28	Rh6G
Water (pH 7)	57	54	55
Methanol (pH 7)	49	47	46
Ethanol (pH 7)	47	45	44
Water (pH 3)	87	84	88
Water/Methanol (93:7 v/v) (pH 3)	96	95	97
Water/Ethanol (93:7 v/v) (pH 3)	95	93	96

[a] Desorption condition: T=25 °C, time = 70 minutes, adsorbent amount=0.50 g, and desorption eluent volume = 100 mL, ternary system

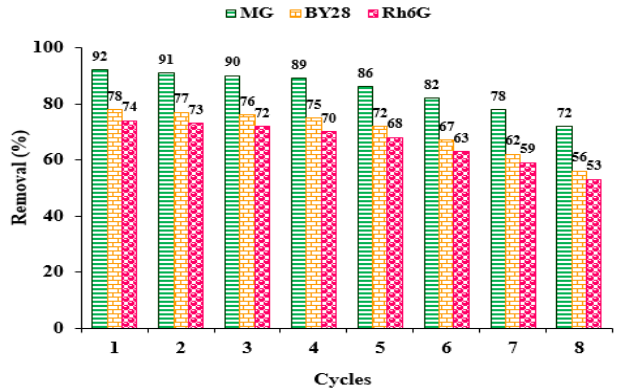

Fig. 15: Removal efficiencies of MG, BY28 and Rh6G dyes in ternary system under several consecutive cycles at optimized condition

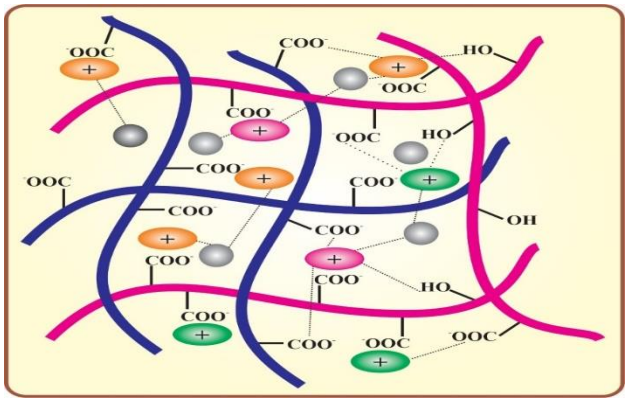

Fig. 16: Possible adsorption mechanism of MG, BY28 and Rh6G cationic dyes onto/into the TG-g-PAA/Fe$_3$O$_4$ hydrogel

Regeneration and reusability study

In industrial process, regeneration and re-usability of an adsorbent is an important stage from economic and industrial pointes of views. The desorption ability of the TG-*g*-PAA/Fe_3O_4 hydrogel was assessed in various solvents (Equation (10)), and the results obtained are presented in Table 5.

$$\text{Desorption (\%)} = \frac{\text{Amount of dye liberated by acid}}{\text{Amount of dye in the adsorbent}} \times 100 \quad (10)$$

As experiment results, the mixture of water/methanol (93/7 v/v) at pH 3 showed the highest desorption efficiency. According to chemical composition of adsorbent, at acidic condition (pH 3) the carboxylic acid groups of hydrogel (more especially PAA segments) are fully protonated that resulted to weaken physical interactions (*e.g.*, ionic) and facilitate desorption of cationic dyes from adsorbent.

The regeneration of the adsorbent was achieved through desorption process as mentioned above, and then the adsorbent was taken for several adsorption–desorption cycles under optimized condition in ternary system. As illustrated in Fig. 15, the removal efficiency of MG, BY28 and Rh6G dyes using TG-*g*-PAA/Fe_3O_4 hydrogel almost remains the same for the first four cycles, after which the removal efficiency decreased gradually owing to saturation of the adsorbent surface that led to the decrease in the availability of attaching sites [54].

Adsorption mechanism

As the chemical composition of TG-*g*-PAA/Fe_3O_4 hydrogel, the electrostatic interactions (*e.g.*, hydrogen bonding and ionic) between the polymeric matrix as well as Fe_3O_4 NPs and dyes are the main physicochemical reason for the adsorption of MG, BY28 and Rh6G cationic dyes. In addition, π-π stacking as well as hydrogen bonding interactions may occur between dyes as their chemical structures (Fig. 16).

Removal efficiency comparison

The removal efficiencies of TG-*g*-PAA/Fe_3O_4 hydrogel in the removal of MG, BY28 and Rh6G dyes was compared with some other sorbents (Table 6). As seen, the TG-*g*-PAA/Fe_3O_4 hydrogel has acceptable Q_m in comparison with others.

Table 6: Comparison of the Q_{max} (mg/g) of other adsorbents in removal of MG, BY28 and Rh6G dyes in ternary system

Adsorbent	Dyes				
	MG	BY28	Rh6G	Q_m (mg/g)	References
Akash Kinari coal	+	-	-	83.42	[53]
Copper sulfide nanoparticles	+	-	-	253.2	[55]
Expanded polystyrene foam	+	-	-	1197.3	[56]
Acid-treated Sawdust	+	-	-	25	[57]
Natural safiot clay	-	+	-	166	[58]
TG-*g*-PAA/Fe_3O_4 hydrogel	+	+	+	626.5/568.2/459.7	This work

CONCLUSIONS

The performance of TG-*g*-PAA/Fe_3O_4 hydrogel in the removal of MG, BY28 and Rh6G dyes from simulated industerial single, binary and ternery systems were investigated, and the most important affacted parametres such as pH, adsorbent amount, contact time, and initial dyes concentrations were optimized. The adsorption isotherm for MG, BY28 and Rh6G dyes by TG-*g*-PAA/Fe_3O_4 hydrogel were investigated by Langmuir and Freundlich models, and it was revelead that the adsorption of all dyes in all systems well-fitted with the Langmuir adsorption isotherm model, which proved the linearity of the adsorption process. The Q_m values for MG, BY28 and Rh6G dyes were quantified for single, bineray and ternary systems. In ternary system, the Q_m values were obtained to be 626.5, 568.2, and 459.7 mg/g, respectively.

In addition, it was revealed that the adsorption process in all systems and for all dyes were best-fitted with the pseudo-second-order model that proved the rate-limiting step might be the adsorption step. The dyes-loaded hydrogel was regenerated through desorption process by mixed water/methanol (93/7 v/v; pH 3), and then reused for several times. It was revealed that the removal performance almost remains the same for the first four cycles, and then decreased gradually.

As the results, it could be conclude that owing to high adsorption capacity of adsorbent, mild process condition (*e.g.*, pH 7 and 25 °C), as well as low cost and eco-friendly nature of adsorbent the TG-*g*-PAA/Fe_3O_4 hydrogel can be applied for efficient removal of mixed cationic dyes from industrial effluents.

Acknowledgements

The authors wish to acknowledge the technical supports from Kermanshah University of Medical Sciences, Kermanshah, Iran.

Received : Oct.14, 2022 ; Accepted : Jan.16, 2023

REFERENCES

[1] Crini G., Kinetic and Equilibrium Studies on the Removal of Cationic Dyes from Aqueous Solution by Adsorption onto a Cyclodextrin Polymer, *Dyes. Pigments.*, **77**: 415-26 (2008).

[2] Deniz F., Kepekci R.A., Bioremoval of Malachite Green from Water Sample by Forestry Waste Mixture as Potential Biosorbent, *Microchem. J.*, **132**: 172-8 (2017).

[3] Machado F.M., Bergmann C.P., Fernandes T.H., Lima E.C., Royer B., Calvete Faganc T.S.B., Adsorption of Reactive Red M-2BE Dye from Water Solutions by Multi-Walled Carbon Nanotubes and Activated Carbon, *J. Hazard. Mater.*, **192**: 1122-1131 (2011).

[4] Machado F.M., Bergmann C.P., Lima E.C., Royer B., de Souza F.E., Jauris I.M., Calveted T.B., Fagan S., Adsorption of Reactive Blue 4 Dye from Water Solutions by Carbon Nanotubes: Experiment and Theory, *Phys. Chem. Chem. Phys.*, **14**: 11139-11153 (2012).

[5] Khan S.A., Abbasi N., Hussain D., Khan T.A., Sustainable Mitigation of Paracetamol with a Novel Dual-Functionalized Pullulan/Kaolin Hydrogel Nanocomposite from Simulated Wastewater, *Langmuir*, **38**: 8280-8295 (2022).

[6] Mohammad-Rezaei R., Khalilzadeh B., Rahimi F., Rezaee P., Shahriar Arab S., Derakhshankhah H., Jaymand M., Simultaneous Removal of Cationic Dyes from Simulated Industrial Wastewater Using Sulfated Alginate Microparticles, *J. Molecul. Liquids.*, **363**: 119880 (2022).

[7] Mohammad-Rezaei R., Khalilzadeh B., Rahimi F., Moradi S., Shahlaei M., Derakhshankhah H., Jaymand M., Simultaneous Removal of Cationic and Anionic Dyes from Simulated Industrial Effluents Using a Nature-Inspired Adsorbent, *Environ. Res.*, **214**: 113966 (2022).

[8] Zeng H., Yu Z., Shao L., Li X., Zhu M., Liu Y., Feng X., Zhu X., A Novel Strategy for Enhancing the Performance of Membranes for Dyes Separation: Embedding PAA@ UiO-66-NH_2 Between Graphene Oxide Sheets, *Chem. Eng. J.*, **403**: 126281 (2021).

[9] Wang H., Li Z., Yahyaoui S., Hanafy H., Seliem M.K., Bonilla-Petriciolet A., Luiz G., Lotfi D., QunLia S., Effective Adsorption of Dyes on an Activated Carbon Prepared from Carboxymethyl Cellulose: Experiments, Characterization and Advanced Modelling, *Chem. Eng. J.*, **417**: 128116 (2021).

[10] Xu L., Pan C., Li S., Yin C., Zhu J., Pan Y., Feng A., Electrostatic Self-Assembly Synthesis of Three-Dimensional Mesoporous Lepidocrocite-Type Layered Sodium Titanate as a Superior Adsorbent for Selective Removal of Cationic Dyes *via* an Ion-Exchange Mechanism, *Langmuir*, **37 (19)**: 6080–6095 (2021).

[11] Kiwaan H., Atwee T., Azab E., El-Bindary A., Photocatalytic Degradation of Organic Dyes in the Presence of Nanostructured Titanium Dioxide, *J. Molecul. Struc.*, **1200**: 127115 (2020).

[12] Demissie H., An G., Jiao R., Ritigala T., Lu S., Wang D., Modification of High Content Nanocluster-Based Coagulation for Rapid Removal of dye from Water and the Mechanism, *Sep. Pur. Technol.*, **259**: 117845 (2021).

[13] Alderete B.L., da Silva J., Godoi R., da Silva F.R., Taffarel S.R., da Silva L.P., Hilario Garciaa A.L., Júniorc H.M., de Amorimd H.L.N., Picadaa J.N. Evaluation of Toxicity and Mutagenicity of a Synthetic Effluent Containing azo dye after Advanced Oxidation Process Treatment, *Chemosphere*, **263**: 128291 (2021).

[14] Lu J., Ayele B.A., Liu X., Chen Q., Electrochemical Removal of RRX-3B in Residual Dyeing Liquid with Typical Engineered Carbonaceous Cathodes, *J. Environ. Manag.*, **280**: 111669 (2021).

[15] Mishra S., Cheng L., Maiti A., The Utilization of Agro-Biomass/Byproducts for Effective Bio-Removal of Dyes From Dyeing Wastewater: A Comprehensive Review, *J. Environ. Chem. Eng.*, **9**: 104901 (2021).

[16] Verma M., Tyagi I., Kumar V., Goel S., Vaya D., Kim H., Fabrication of GO–MnO_2 Nanocomposite Using Hydrothermal Process for Cationic and Anionic Dyes Adsorption: Kinetics, Isotherm, and Reusability, *J. Environ. Chem. Eng.*, **9**: 106045 (2021).

[17] Abdulhameed A.S., Hum N.N.M.F., Rangabhashiyam S., Jawad A.H., Wilson L.D., Yaseen Z.M., Al-Kahtanif A.A., Al-Kahtanif Z.A.A., Statistical Modeling and Mechanistic Pathway for Methylene Blue dye Removal by High Surface Area and Mesoporous Grass-Based Activated Carbon Using K_2CO_3 Activator, *J. Environ. Chem. Eng.*, **9**: 105530 (2021).

[18] Pishnamazi M., Khan A., Kurniawan T.A., Sanaeepur H., Albadarin A.B., Soltani R., Adsorption of Dyes on Multifunctionalized Nano-Silica KCC-1, *J. Molecul. Liquids.*, **338**: 116573 (2021).

[19] Usman M., Ahmed A., Yu B., Wang S., Shen Y., Cong H., Simultaneous Adsorption of Heavy Metals and Organic Dyes by β-Cyclodextrin-Chitosan Based Cross-Linked Adsorbent, *Carbohyd. Polym.*, **255**: 117486 (2021).

[20] Toumi I., Djelad H., Chouli F., Benyoucef A., Synthesis of PANI@ZnO Hybrid Material and Evaluations in Adsorption of Congo Red and Methylene Blue Dyes: Structural Characterization and Adsorption Performance, *J. Inorg. Organometal. Polym. Mater.*, **32**: 112-121 (2022).

[21] Hajiaghababaei L., Ashrafi L., Dehghan Abkenar S., Badiei A., Ganjali MR., Mohammadi Ziarani G., Efficient Removal of Reactive Blue-19 from Textile Wastewater by Adsorption on Methyl Imidazolium Modified LUS-1 and MCM-48 Nanoporous, *Int. J. Nano Dimension.*, **11**: 237-247 (2020).

[22] Habibi S., Hajiaghababaei L., Badiei A., Yadavi M., Abkenar S.D., Ganjali M.R., Ziarani G.M., Removal of Reactive Black 5 from Water Using Carboxylic Acid-Grafted SBA-15 Nanorods, *Desalin. Water. Treat.*, **95**: 333-341 (2017).

[23] Wang G.Q., Huang J.F., Huang X.F., Deng S.Q., Zheng S.R., Cai S.L., Fan J., Zhanga W.Z., A Hydrolytically Stable Cage-Based Metal–Organic Framework Containing Two Types of Building Blocks for the Adsorption of Iodine and Dyes, *Inorg. Chem. Front.*, **8**: 1083-1092 (2021).

[24] Jaymand M., Sulfur Functionality-Modified Starches: Review of Synthesis Strategies, Properties, and Applications, *Int. J. Biol. Macromol.*, **197**: 111-120 (2022).

[25] Safarzadeh Kozani P., Safarzadeh Kozani P., Hamidi M., Valentine Okoro O., Eskandani M., Jaymand M., Polysaccharide-Based Hydrogels: Properties, Advantages, Challenges, and Optimization Methods for Applications in Regenerative Medicine, *Int. J. Polym. Mater. Polym. Biomater.*, **17**: 1319-1333 (2022).

[26] Li P., Wang T., He J., Jiang J., Lei F., Synthesis, Characterization, and Selective dye Adsorption by pH- and Ion-Sensitive Polyelectrolyte Galactomannan-Based Hydrogels, *Carbohyd. Polym.*, **264**: 118009 (2021).

[27] Nayak S., Prasad SR., Mandal D., Das P., Carbon Dot Cross-Linked Polyvinylpyrrolidone Hybrid Hydrogel for Simultaneous Dye Adsorption, Photodegradation and Bacterial Elimination from Waste Water, *J. Hazard. Mater.*, **392**: 122287 (2020).

[28] Khan S.A., Hussain D., Abbasi N., Khan T.A., Deciphering the Adsorption Potential of a Functionalized Green Hydrogel Nanocomposite for Aspartame from Aqueous Phase, *Chemosphere*, **289**: 133232 (2022).

[29] Soleimani K., Derakhshankhah H., Jaymand M., Samadian H., Stimuli-Responsive Natural Gums-Based Drug Delivery Systems for Cancer Treatment, *Carbohyd. Polym.*, **254**: 117422 (2021).

[30] Qi X., Wu L., Su T., Zhang J., Dong W., Polysaccharide-Based Cationic Hydrogels for Dye Adsorption, *Colloids Surfaces B.*, **170**: 364-72 (2018).

[31] Pereira A.G.B., Rodrigues F.H.A., Paulino A.T., Martins A.F., Fajardo A.R., Recent Advances on Composite Hydrogels Designed for the Remediation of Dye-Contaminated Water and Wastewater: A Review, *J. Clean. Product.*, **284**: 124703 (2021).

[32] Verbeken D., Dierckx S., Dewettinck K., Exudate Gums: Occurrence, Production, and Applications, *Appl. Microb. Biotechnol.*, **63**: 10-21 (2003).

[33] Hong K.H., Oh K.W., Kang T.J., Preparation of Conducting Nylon-6 Electrospun Fiber Webs by the in Situ Polymerization of Polyaniline, *J. Appl. Polym. Sci.*, **96**: 983-991 (2005).

[34] Hosseini M.S., Hemmati K., Ghaemy M., Synthesis of Nanohydrogels Based on Tragacanth Gum Biopolymer and Investigation of Swelling and Drug Delivery, *Int. J. Biol. Macromol.*, **82**: 806-815 (2016).

[35] Nejatian M., Abbasi S., Azarikia F., Gum Tragacanth: Structure, Characteristics and Applications in Foods, *Int. J. Biol. Macromol.*, **160**: 846-860 (2020).

[36] Ghaderi-Ghahfarokhi M., Yousefvand A., Ahmadi Gavlighi H., Zarei M., Farhangnia P., Developing Novel Synbiotic Low-Fat Yogurt with Fucoxylogalacturonan from Tragacanth Gum: Investigation of Quality Parameters and Lactobacillus Casei Survival, *Food. Sci. Nutrition.*, **8**: 4491-4504 (2020).

[37] Hemmati K., Masoumi A., Ghaemy M., Tragacanth Gum-Based Nanogel as a Superparamagnetic Molecularly Imprinted Polymer for Quercetin Recognition and Controlled Release, *Carbohyd. Polym.*, **136**: 630-640 (2016).

[38] Zare E.N., Makvandi P., Tay F.R., Recent Progress in the Industrial and Biomedical Applications of Tragacanth Gum: A Review, *Carbohyd. Polym.*, **212**: 450-467 (2019).

[39] Sayadnia S., Arkan E., Jahanban-Esfahlan R., Sayadnia S., Jaymand M., Thermal-Responsive Magnetic Hydrogels Based on Tragacanth Gum for Delivery of Anticancer Drugs, *J. Polym. Res.*, **28**: 1-13 (2021).

[40] Sadeghi S., Moghaddam A.Z., Massinaei M., Novel Tunable Composites Based on Bentonite and Modified Tragacanth Gum for Removal of Acid Dyes from Aqueous Solutions, *RSC Adv.*, **5**: 55731-55745 (2015).

[41] Mallakpour S., Tabesh F., Tragacanth Gum Based Hydrogel Nanocomposites for the Adsorption of Methylene Blue: Comparison of Linear and Non-Linear forms of Different Adsorption Isotherm and Kinetics Models, *Int. J. Biol. Macromol.*, **133**: 754-766 (2019).

[42] Chen X., Huang Z., Luo S.Y., Zong M.H., Lou W.Y., Multi-Functional Magnetic Hydrogels Based on Millettia Speciosa Champ Residue Cellulose and Chitosan: Highly Efficient and Reusable Adsorbent for Congo Red and Cu^{2+} Removal, *Chem. Eng. J.*, **423**: 130198 (2021).

[43] Wu S., Guo J., Wang Y., Huang C., Hu Y., Facile Preparation of Magnetic Sodium Alginate/Carboxymethyl Cellulose Composite Hydrogel for Removal of Heavy Metal Ions from Aqueous Solution, *J. Mater. Sci.*, **56**: 13096-13107 (2021).

[44] Zhou Y., Wang Y., Dong S., Hao H., Li J., Liu C., Li X., Tong Y., Phosphate Removal by a La $(OH)_3$ Loaded Magnetic MAPTAC-Based Cationic Hydrogel: Enhanced Surface Charge Density and Donnan Membrane Effect, *J. Environ. Sci.*, **113**: 26-39 (2022).

[45] Fazilati A., Mokhtarian N., Latifi A.M., Fazilati M., Synthesis of Acrylic Acid Polymer Hydrogel Nano Fe_3O_4 to Remove Ammonia from Sugarcane Field Waste, *Adv. Mater. Sci. Eng.*, **9204523**: (2020).

[46] Tiwari A., Bind A., Adsorption of Pesticide (Captan) Onto Super Paramagnetic Poly (Styrene-Co-Acrylic Acid) Hydrogel from Aqueous Solution Using Batch and Column Studies, *Anal. Chem. Lett.*, **4**: 267-278 (2014).

[47] Sayadnia S., Arkan E., Jahanban-Esfahlan R., Sayadnia S., Jaymand M., Tragacanth Gum-Based pH-Responsive Magnetic Hydrogels for "Smart" Chemo/Hyperthermia Therapy of Solid Tumors, *Polym. Adv. Technol.*, **32**: 262-271 (2021).

[48] Derakhshankhah H., Haghshenas B., Eskandani M., Jahanban-Esfahlan R., Abbasi-Maleki S., Jaymand M., Folate-Conjugated Thermal- and pH-Responsive Magnetic Hydrogel as a Drug Delivery Nano-System for "Smart" Chemo/Hyperthermia Therapy of Solid Tumors, *Mater. Today. Commun.*, **30:** 103148 (2022).

[49] Shenvi S.S., Isloor A.M., Ismail A.F., Shilton S.J., Al Ahmed A., Humic Acid Based Biopolymeric Membrane for Effective Removal of Methylene Blue and Rhodamine B, *Indust. Eng. Chem. Res.*, **54**: 4965-4975 (2015).

[50] Preethi S., Sivasamy A., Sivanesan S., Ramamurthi V., Swaminathan G., Removal of Safranin Basic Dye from Aqueous Solutions by Adsorption onto Corncob Activated Carbon, *Indust. Eng. Chem. Res.*, **45**: 7627-7632 (2006).

[51] Vafaei MA., Shakeri A., Salehi H., Razavi SR., Salari N., The Effect of Nanosheets on Polymer Hydrogels Performance in Rhodamine B Dye Removal by Forward Osmosis Process, *J. Water. Proces. Eng.* **44**: 102351 (2021).

[52] Wang W., Wang J., Zhao Y., Bai H., Huang M., Zhang T., Song S., High-Performance Two-Dimensional Montmorillonite Supported-Poly (Acrylamide-Co-Acrylic Acid) Hydrogel for Dye Removal, *Environ. Pollution.*, **257**: 113574 (2020).

[53] Khan T.A., Singh V.V., Kumar D., Removal of Some Basic Dyes from Artificial Textile Wastewater by Adsorption on Akash Kinari Coal, **63**: 355-364 (2004).

[54] Wadhera P., Jindal R., Dogra R., Synthesis of Semi Interpenetrating Network Hydrogel [(GrA-Psy)-cl-Poly (AA)] and its Application for Efficient Removal of Malachite Green from Aqueous Solution, *Polym. Eng. Sci.*, **59**: 1416-1427 (2019).

[55] Bagheri A.R., Ghaedi M., Asfaram A., Hajati S., Ghaedi A.M., Bazrafshan A., Rahimi M.R., Modeling and Optimization of Simultaneous Removal of Ternary Dyes onto Copper Sulfide Nanoparticles Loaded on Activated Carbon Using Second-Derivative Spectrophotometry, *J. Taiwan. Institute. Chem. Eng.*, **65**: 212-224 (2016).

[56] Li W., Xie Z., Xue S., Ye H., Liu M., Shi W., Liu Y., Studies on the Adsorption of Dyes, Methylene Blue, Safranin T, and Malachite Green onto Polystyrene Foam. *Sep. Pur.Technol.*, **276**: 119435 (2021).

[57] Adebisi A.R., Ayanpeju G.K., Wewers A.F., Oladipo M.A., Removal of Malachite Green from Single and Multi-Dye Aqueous Solutions by Acid-Treated Sawdust, *Orient. J. Chem.*, **35**: 1384 (2019).

[58] El Kassimi A., Boutouil A., El Himri M., Laamari M.R., El Haddad M., Selective and Competitive Removal of three Basic Dyes from Single, Binary and Ternary Systems in Aqueous Solutions: A Combined Experimental and Theoretical Study, *J. Saudi. Chem. Soc.*, **24**: 527-544 (2020).